PERFORMANCE EVALUATION OF ACCIDENT TOLERANT FUEL CLADDINGS DURING SEVERE ACCIDENTS OF BWRS

T. IKEGAWA,[1] T. KONDO,[1]
[1] *Nuclear Plant Engineering Department, Hitachi-GE Nuclear Energy, Ltd., 1-1, Saiwai-cho, 3-chome, Hitachi-shi, Ibaraki 317-0073, Japan*

K. SAKAMOTO,[2] S. YAMASHITA,[3]
[2] *Nippon Nuclear Fuel Development Co., Ltd. (NFD), Oarai-machi, Ibaraki 311-1313, Japan*
[3] *Japan Atomic Energy Agency (JAEA), Tokai-mura, Ibaraki 319-1195, Japan*

ABSTRACT

SiC/SiC composite and FeCrAl-oxide dispersion strengthened (ODS) steel are promising candidate accident tolerant fuel (ATF) materials for light water reactor claddings. Performance was evaluated for two representative accident sequence groups of the advanced boiling water reactor, traditionally called as TQUV and TB. The TQUV assumes that high pressure water injection fails, depressurisation is successful, and low pressure water injection fails; therefore, the core is damaged at an early timing under a low pressure condition. The TB is a station blackout. In the TB, a reactor core isolation cooling (RCIC) successfully cools the core for several days and after RCIC water injection is stopped, the core is damaged at a late timing under a high pressure condition. The results obtained by the latest MAAP code (ver.5.05β) showed that the steam-caused oxidation reaction was effectively suppressed by using ATFs instead of conventional Zircaloy (Zry). Sensitivity analysis was performed for the TB to investigate the performance of ATFs with accident management. The results showed that the depressurisation timing could be delayed 0.5-3.0h by using ATFs, and that the minimum water injection flow rate to prevent core damage could be decreased by about a half compared with conventional Zry.

1. Introduction

In the 2011 Fukushima Daiichi Nuclear Power Plant (FDNPP) accident, hydrogen explosions occurred in the operating floors of Unit-1, Unit-3, and Unit-4 reactor buildings. The primary hydrogen source for these explosions has still not been completely identified because there would be several sources such as the steam-caused oxidation reaction (hereinafter called steam oxidation reaction) of fuel cladding in the core, the water-caused oxidation reaction at the surface of molten core that fell into the water pool of the lower plenum located below the core, and the molten core-concrete interaction (MCCI) which may occur in the lower drywell located below the reactor pressure vessel (RPV). One of the most important lesson-learnt issues from the FDNPP accident is to suppress the steam oxidation reaction of fuel cladding in the core to prevent core damage while accident management (AM) measures are conducted. SiC/SiC composite (hereinafter called SiC) and FeCrAl-ODS steel (hereinafter called ODS) are promising candidates for accident tolerant fuel (ATF) materials for light water reactor claddings since they have excellent resistance to high temperature steam. A lot of severe accident (SA) analyses for pressurised water reactors (PWRs) and boiling water reactors (BWRs) have been conducted worldwide [1]-[8]. Those analyses showed that core damage may be prevented by applying ATFs instead of conventional Zircaloy (Zry). In the present study, the ATF performance in accidents was investigated by the latest version of the MAAP code (MAAP5.05β) for the advanced BWR (ABWR). Two kinds of SA analysis were performed: one with AM and the other without AM.

2. Analysis conditions

2.1 Analysis code

The Modular Accident Analysis Program (MAAP) [9] is one of the most commonly used computer codes to evaluate plant status during a SA. MAAP was originally developed in the

IDCOR (Industry Degraded Core Rulemaking) Program, and the first product was released in the 1980s. The Electric Power Research Institute (EPRI) in the U.S. currently owns the code, and it has continued to be revised.
MAAP code can evaluate each stage of SA progression such as core melt, RPV failure, primary containment vessel (PCV) failure, etc. MAAP has physics models for the phenomena which could occur during an accident in the core, primary system, and containment and it has models of systems which can be used for preventing or mitigating accidents. Thus, it allows the effectiveness of engineered safety features and other systems to be evaluated to prevent or mitigate the progression of beyond design basis accidents. MAAP can also treat fission product behaviours which are important for evaluation of the source term. Therefore, MAAP can treat a wide range of the important phenomena during accidents and it can calculate phenomena from any of the initiating events until safe and stable conditions are reached or until PCV failure occurs due to overpressure or overtemperature, etc.
MAAP solves mass and energy conservation equations with sufficient accuracy. On the other hand, the momentum equation is approximately treated with an assumption of the quasi-steady state. Because of this assumption, MAAP cannot evaluate very fast flow phenomena precisely such as the containment flow condition just after loss of coolant accidents (LOCAs) occur. However, MAAP has sufficient applicability for SAs which have relatively long period phenomena compared to LOCAs.
Now, the MAAP code Ver.5.05 is being developed by the EPRI to handle ATF in addition to conventional Zry. A beta version of MAAP5.05 (MAAP5.05β) was released to the MAAP User's group, however presently it has the limitation that it can handle ATF behaviour only inside the core. In this study, MAAP5.05β was used and ATF performance until fuel cladding failure was investigated.

2.2 Material properties

Tab 1 shows material properties of the ATFs used for the SA analysis. Conventional UO_2 fuels with the ATF claddings (i.e. claddings made of the ATFs) were investigated.

Tab 1: Material properties of the ATFs

Item	SiC/SiC composite (SiC)	FeCrAl-ODS steel (ODS)
Density (kg/m^3)	2900	Fig 1.
Specific heat (J/kgK)	Eq. (1)	Fig 1.
Thermal conductivity (W/mK)	25	Fig 1.
Melting point (K)	2366*	1773
Reaction model for steam	Eqs. (3), (5), (6)	Eqs. (8), (10)

*: Though the thermal decomposition temperature of SiC is estimated to be 2818K, the melting point of 2366K was used. It was calculated as the eutectic temperature of SiC and UO_2 using the Thermo-Calc Software with the NUCL10 database.

Specific heat of SiC was calculated by the following correlation [10]:

$$C_p = 925.65 + 0.3772T - 7.9259\times10^{-5}T^2 - 3.1946\times10^{7}T^{-2} \cdots (1)$$

where C_p is specific heat of SiC (J/kgK), T is temperature (K).
It is important for SA analysis to consider steam oxidation reaction of fuel cladding because it occurs at high temperature and a large amount of hydrogen may be generated during an accident. In the case of SiC, two kinds of reactions are known to occur at high temperature, the steam oxidation reaction and the oxide (SiO_2) volatilisation reaction. The following correlations introduced by the Oak Ridge National Laboratory (ORNL) [11] were used for this study.

1) Steam oxidation reaction
When exposed to steam, SiC forms SiO_2 via the following reaction.

$$SiC + 3H_2O \rightarrow SiO_2 + 3H_2 + CO \quad \cdots (2)$$

The kinetics of SiO_2 growth in the absence of any volatilisation is controlled by diffusion of the oxidising species through the SiO_2 film (parabolic kinetics). The parabolic oxidation rate constant (k_p) was obtained by the ORNL [11] as:

$$k_p[mg^2/cm^4h] = p \cdot \exp\left(14.13 \pm 3.7 + \frac{-238 \pm 53}{R \cdot T}\right) \quad \cdots (3)$$

where p is pressure (MPa), R is the gas constant (kJ/molK), and T is temperature (K). The heat of the reaction (Eq. (2)) was set at 206kJ/mol (exothermic reaction).

2) Oxide film volatilisation reaction

In the presence of steam, SiC undergoes volatilisation via the following reaction.

$$SiO_2 + 2H_2O \rightarrow Si(OH)_4 \quad \cdots (4)$$

The high pressure and atmospheric pressure linear volatilisation rate constants are summarised in Eqs. (5) and (6) for high-pressure and low-pressure steam conditions, respectively.

(i) 0.34 – 2.0MPa (high pressure range) [11]

$$k_l[mg/cm^2h] = v^{0.5} \cdot p^{1.5} \cdot \exp\left(19.6 \pm 3.2 + \frac{-211 \pm 40}{R \cdot T}\right) \quad \cdots (5)$$

(ii) 0.1MPa (low pressure range) [11]

$$k_l[mg/cm^2h] = v^{0.5} \cdot p^{1.5} \cdot \exp\left(9.7 \pm 1.3 + \frac{-123 \pm 18}{R \cdot T}\right) \quad \cdots (6)$$

Where v is gas velocity (m/s). Heat of the reaction (Eq. (4)) was set at -56kJ/mol (endothermic reaction).

In the case of ODS, the density, specific heat, and thermal conductivity shown in **Fig 1** were used for the analysis [12].

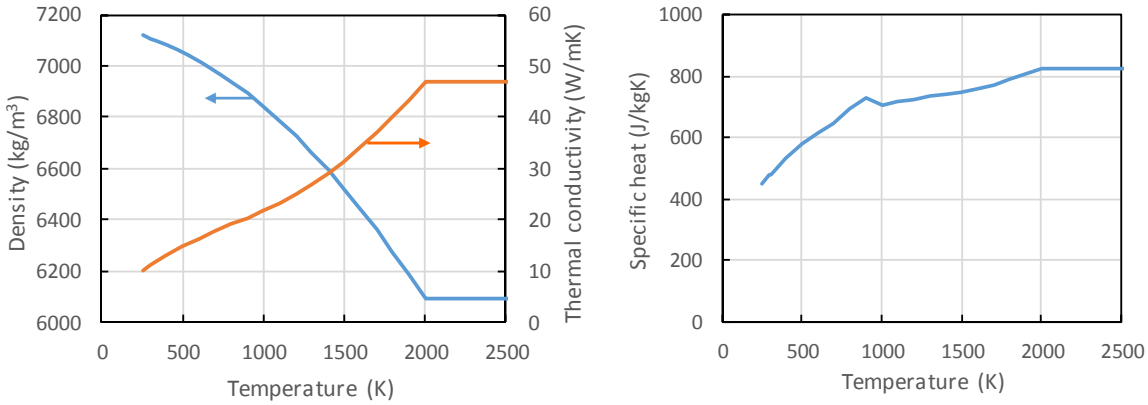

Fig 1. FeCrAl-ODS steel (ODS) properties

The oxide film volatilisation reaction does not need to be considered for ODS because the oxide film does not react with steam. However, two kinds of steam oxidation reactions have to be considered for ODS for two kinds of oxide generation, Al_2O_3 and $FeO \cdot Cr_2O_3$. In the case of the low steam temperature region (<Al_2O_3 film failure temperature), the steam oxidation reaction for Al_2O_3 has to be used, and the other steam oxidation reaction for $FeO \cdot Cr_2O_3$ has to be used in the high steam temperature region because Al_2O_3 film no longer protects the material surface and Fe and Cr are oxidized by high temperature steam directly.

1) Al oxidation reaction

Al_2O_3 is generated by the following steam oxidation reaction.

$$Al + \frac{3}{2}H_2O \rightarrow \frac{1}{2}Al_2O_3 + \frac{3}{2}H_2 \quad \cdots (7)$$

The kinetics of Al_2O_3 growth is controlled by diffusion of the oxidising species through the Al_2O_3 film (parabolic kinetics). The parabolic oxidation rate constant (k_p) was evaluated from the Kanthal APMT [13] as:

$$k_p\left(Al_2O_3\right) = k_{p0}\left(Al_2O_3\right)\cdot\exp\left(-\frac{Q\left(Al_2O_3\right)}{R\cdot T}\right) \quad \cdots (8)$$

where $k_{p0}(Al_2O_3)$ is 784.0kg^2/m^{4}s and $Q(Al_2O_3)$ is 344kJ/mol. Heat of the reaction was set at 464kJ/mol (exothermic reaction). Since Al_2O_3 film strongly suppresses additional fuel cladding oxidation and hydrogen generation, ODS has an excellent property for preventing fuel failure due to the temperature increase by heat of the reaction.

2) FeCr oxidation reaction

The steam oxidation reaction of FeCr was represented by the following equation.

$$Fe + 2Cr + 4H_2O \rightarrow FeO\cdot Cr_2O_3 + 4H_2 \quad \cdots (9)$$

The parabolic oxidation rate constant (k_p) was calculated by the following correlation. The original MAAP values for stainless steel were used for the two constants ($k_{p0}(FeO\cdot Cr_2O_3)$, $Q(FeO\cdot Cr_2O_3)$) [9]. Heat of the reaction was set at 47kJ/mol (exothermic reaction). In this study, since Al_2O_3 film failure temperature was assumed to be the same as the ODS melting temperature of 1773K, the steam oxidation reaction for $FeO\cdot Cr_2O_3$ was not substantially used for the analysis conducted in this study.

$$k_p\left(FeO\cdot Cr_2O_3\right) = k_{p0}\left(FeO\cdot Cr_2O_3\right)\cdot\exp\left(-\frac{Q\left(FeO\cdot Cr_2O_3\right)}{R\cdot T}\right) \quad \cdots (10)$$

2.3 Analysis conditions

Tab 2 shows analysis conditions of this study. The ABWR was selected as the latest commercial BWR. Step III type fuel assemblies (9×9) were assumed to be loaded in the ABWR core. Thermal output and RPV dome pressure were set at 3926MWt and 7.07MPa[g] respectively as nominal operating conditions. Initial water level in the RPV was assumed to be the normal water level. Three kinds of analyses were performed for fuel cladding and channel box (C/B) materials (the Zry, SiC, and ODS) to confirm advantages of the ATFs. The core was divided by a cylindrical coordinate system, and the numbers of axial and radial nodes were 30 and 5, respectively. Cladding failure temperatures for the Zry, SiC, and ODS were assumed as 2500, 2366, and 1773K, respectively. Though the cladding failure temperature of the Zry may be 2911K (melting point of ZrO_2), 2500K was applied in consideration of other failure mechanisms besides melting such as brittle fracture of ZrO_2 due to flow induced vibration, etc.

Tab 2: Analysis conditions

Item	Value
Plant type	ABWR
Fuel type	9×9 (Step III)
Thermal output	3926MWt
RPV dome pressure	7.07MPa[g]
Initial water level in the RPV	Normal level
Materials of cladding and C/B	Zry, SiC/SiC composite (SiC), and FeCrAl-ODS steel (ODS)
Core nodalisation	Axial: 30 nodes Radial: 5 nodes
Cladding failure temperature	Zry: 2500K SiC: 2366K ODS: 1773K

2.4 Accident sequence groups

Two representative accident sequence groups for the ABWR shown in **Tab 3** were assumed in this study. For the TQUV, loss of all feedwater flow (Q) is assumed as the initiating transient event (T). The RPV is isolated by the main steam isolation valves (MSIVs) to prevent radioactive material release to outside the PCV, and the reactor is tripped by full insertion of all control rods into the core by scram. All high pressure core injection systems, including the feedwater system, control rod drive (CRD) system, and high pressure core flooder (HPCF) fail (H). The automatic depressurisation system (ADS) successfully opens the safety relief valves (SRVs) manually, however low pressure core injection measures including the low pressure core flooder (LPFL) and alternative water injection completely fail (V). As a result, core is damaged due to lack of cooling water at an early timing with low pressure condition because depressurisation by the ADS is assumed to be successful.

The TB means a station blackout (SBO). In the sequence group, loss of off-site power is assumed as the initiating transient event. The reactor is tripped by a scram signal generated by the low turbine power trip (T). The MSIVs are closed due to their trip signal such as loss of the main condenser vacuum. All emergency diesel generators are assumed to fail (B); however power supply by DC batteries are available. Therefore, water is supplied into the core using the reactor core isolation cooling (RCIC) which does not need any AC power supply for activation, and core damage can be prevented during the RCIC activation. However, as recovery of the residual heat removal system (RHR) and water injection measures such the LPFL and alternative water injection are assumed to fail, the RCIC water injection stops due to the DC batteries running out and the core is damaged due to lack of cooling water at a late timing with the high pressure condition because depressurisation by the ADS is assumed to be failed due to lack of DC power. In this study, the water injection period by the RCIC was assumed to be 72h (3days) in consideration of the FDNPP accident.

Tab 3: Accident sequence groups

Name	Events (chronological order)
TQUV	✓ Loss of all feedwater flow. ✓ The MSIVs close and reactor shutdown occurs by scram. ✓ High pressure water injection such as the feedwater, purge flow from the CRD, and HPCF failure. ✓ Successful depressurisation by the ADS. ✓ Low pressure water injections such as by the LPFL and alternative water injection failure. ✓ Core is damaged due to lack of cooling water.
TB	✓ Loss of off-site power. ✓ Reactor shutdown occurs by scram and the MSIVs close. ✓ AC power such as emergency diesel generators failure (DC battery powers are available). ✓ High pressure water injection by the RCIC successful. ✓ Recovery of the RHR and water injections such as LPFL and alternative water injection failure. ✓ The RCIC stops due to the DC batteries running out. ✓ Core is damaged due to lack of cooling water.

2.5 Accident management conditions

Tab 4 shows AM conditions assumed in this study. Since TQUV does not have much time for AM by operators, the long term TB was selected as the representative SA analysis case. Three parameters were selected for sensitivity analysis, water injection period by the RCIC, depressurisation timing after the RCIC stops, and water flow rate after depressurisation. The water injection period by the RCIC affects decay heat level. The less decay heat there is, the more effective ATFs are because heat of the steam oxidation reaction becomes relatively large compared to decay heat. Depressurisation timing is the most important parameter for AM because depressurisation is necessary to inject water into the core by manual water injection measures such as using fire engines. If depressurisation fails, the core will melt because of

the high temperature due to the lack of cooling water even if fire engines can be used. The third parameter (water flow rate after depressurisation) is also important for AM because the low flow rate of water may enhance the steam oxidation reaction rather than cooling the fuel cladding and fuel cladding failure may progress.

Tab 4: AM conditions

Item		Value	Notes
Sequence group		TB	Long term sequence for AM
Parameters	Water injection period by the RCIC	24, 72, 720h	0.6, 0.4, 0.16% (Decay heat)
	Depressurisation timing	2 – 26h after stopping RCIC	2 SRVs are assumed to be open
	Water flow rate	90 – 230m^3/h	Considering Japanese fire engine specifications (90 – 168m^3/h).

3. Analysis results

3.1 SA without AM

Fig 2 shows the TQUV analysis results for Zry, SiC, and ODS. It is noted that the analysis results were shown until fuel cladding failure because of the limitation of MAAP5.05β and further investigations after fuel cladding failure are expected. Peak cladding temperature in the core and the amount of hydrogen generated in the core were clearly mitigated by using the ATFs. Since the steam oxidation reaction rate of the ATFs is relatively smaller than that of Zry, the cladding temperature increase rate of the ATFs could be suppressed effectively. It should be noted that fuel failure timing of ODS was almost the same as that of the conventional Zry though cladding failure temperature of ODS (1773K) is less than that of the Zry (2500K). In the case of SiC, fuel failure timing could be delayed about 0.14h compared with the Zry because cladding failure temperature of SiC was assumed to be 2366K. Since the steam oxidation reaction could be suppressed effectively by applying the ATFs, the amount of hydrogen generated in the core would also be limited and the hydrogen combustion risk inside the reactor building will be decreased by applying the ATFs. Since the TQUV progressed under the low pressure condition because the ADS successfully depressurised the RPV and the oxide film (SiO_2) volatilisation reaction rate constant of Eq. (6) was not large, the steam oxidation reaction and the amount of hydrogen generated in the core of SiC fuel were well-suppressed.

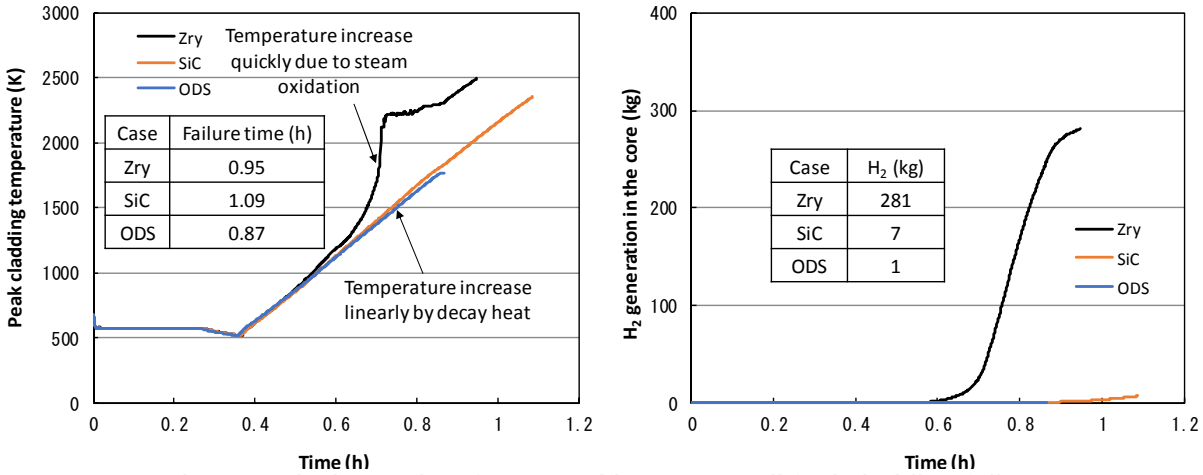

Fig 2. Analysis results of TQUV without AM until fuel cladding failure

Fig 3 shows the TB analysis results for the Zry, SiC, and ODS after stopping the RCIC at 72h. Peak cladding temperature in the core and the amount of hydrogen generated in the core were clearly mitigated by using the ATFs the same as in the TQUV. In this analysis, fuel failure timing of SiC was delayed 1.0h compared with the conventional Zry. Though melting temperature of

ODS was lower than that of Zry, fuel failure timing of ODS could be delayed 0.6h. The amount of hydrogen generated in the core was effectively suppressed by using the ATFs, especially for ODS (about 4kg) because Al_2O_3 film can protect ODS as a hard barrier. On the other hand, some amount of hydrogen was generated in the case of SiC (about 96kg). This was because the TB is high pressure sequence and oxide film (SiO_2) volatilisation rate constant at high pressure (Eq. (5)) is much larger than that at low pressure (Eq. (6)). The effect of oxide film volatilisation reaction on fuel damage timing is discussed in Section 4.

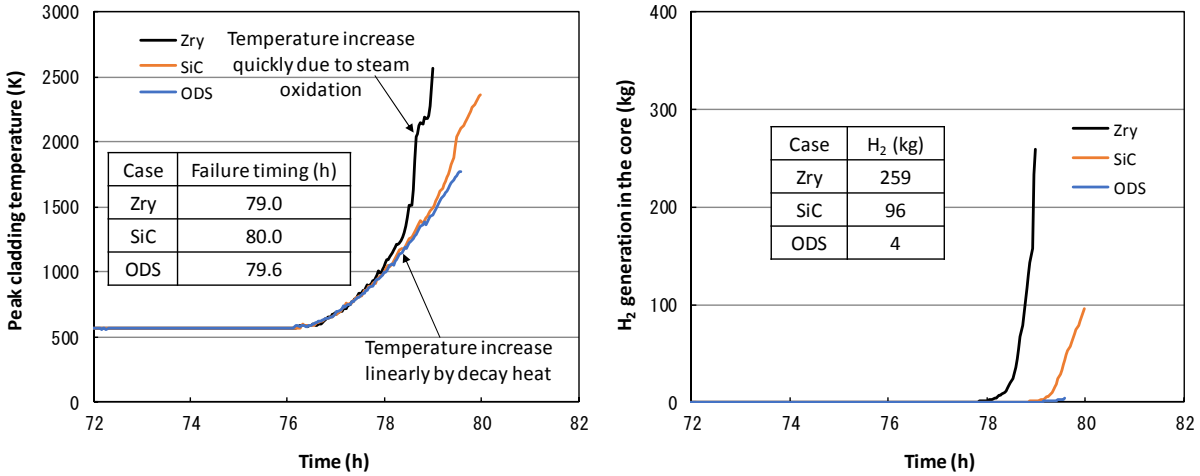

Fig 3. Analysis results of TB without AM until fuel cladding failure

3.2 SA with AM

Fig 4 shows the analysis results of the margin of depressurisation timing to prevent fuel damage. “Margin of depressurisation” means the depressurisation margin differences between the ATFs and conventional Zry, and “depressurisation margin” means the period of depressurisation timing after the RCIC stops which can prevent fuel damage. Therefore, the vertical-axis indicates the ATF performance in the TB with AM.

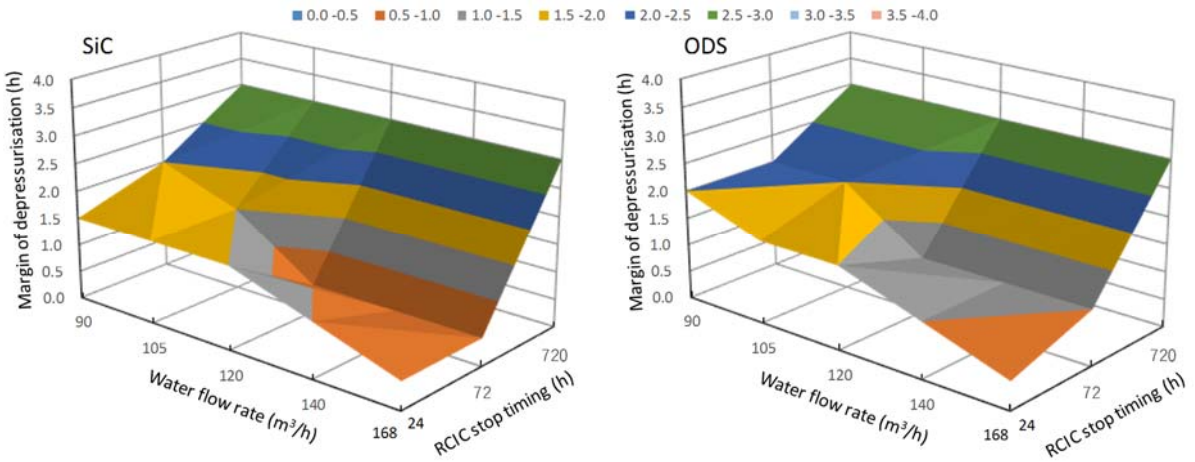

Fig 4. Margin of depressurisation timing for preventing fuel damage with AM

The following tendencies were found when the ATFs were applied to fuel cladding and C/B.

- ✓ Time margin of depressurisation was evaluated in the range of 0.5 - 3.0h.
- ✓ Since the amount of added heat by the steam oxidation reaction by the ATFs was relatively smaller than that by the Zry, the ATF application effect was maximised with a low decay heat level (i.e. 720h) because the total amount of heat (decay heat + additive heat) could decrease.
- ✓ The effect of ATF application was maximised with a low water flow rate (i.e. 90m^3/h) because the ATFs could be cooled effectively even for a small amount of steam though the conventional Zry has a risk that a small amount of steam enhances hydrogen

generation and added heat by the steam oxidation reaction may damage Zry.

✓ Compared with SiC and ODS, ODS has the potential to show a larger margin since the oxide film thickness of SiC, which is a barrier against SiC oxidation, cannot increase sufficiently due to the oxide film volatilisation. This effect is discussed in Section 4.

Fig 5 shows the analysis results of the minimum water flow rates for preventing fuel damage. The minimum water flow rate increased when depressurisation timing was delayed. Compared to Zry, the ATFs demonstrated a potential to prevent core damage with about half the water flow rate. Since SiO_2 thickness cannot increase due to its volatilisation reaction, SiC performance was a little worse than that of ODS. **Fig 6** shows the analysis results for the analysis point shown in **Fig 5** (7h, 90m³/h). The Zry failed quickly because depressurisation timing was too late; however, the ATFs could prevent failure by depressurisation and low flow rate water injection. It should be noted that steam generation by depressurisation (i.e. flashing) could cool the core effectively for the ATFs and that contributed to preventing core damage.

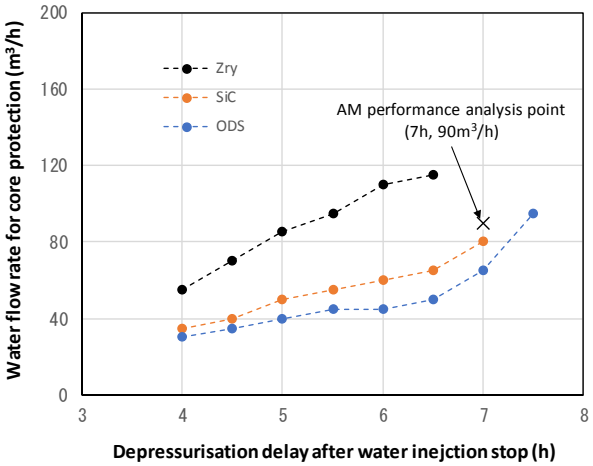

Fig 5. Minimum water flow rate for preventing fuel damage (RCIC stop timing: 72h)

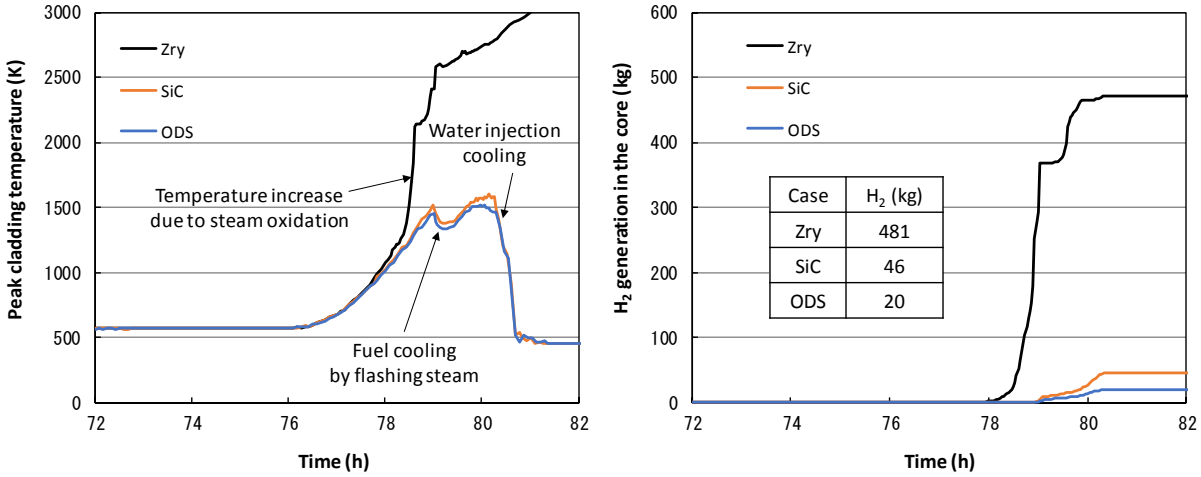

Fig 6. Analysis results of TB with AM
(RCIC stop timing, 72h; depressurisation timing, 7h; water flow rate, 90m³/h)

4. Discussion

4.1 ODS

Though melting temperature of ODS is lower than that of the Zry and SiC, the analysis results for ODS showed excellent performance because the steam oxidation reaction rate constant of Al (Eq. (8)) is small and the generated oxide film (Al_2O_3) is stable even at high temperature. However, it should be noted that the upper temperature limit of Al_2O_3 film stability is an important parameter to prevent the steam oxidation reaction with Fe and Cr. Development of ODS with high Al_2O_3 film stability will be beneficial to improve its performance in accidents.

4.2 SiC

Semi-equilibrium SiO_2 thickness, which means the SiO_2 generation rate by steam oxidation and the SiO_2 volatilisation rate become equal, was estimated to confirm the effect of the volatilisation of SiO_2. The rate of change in SiO_2 thickness is then given by paralinear kinetics [11]:

$$\frac{dx}{dt} = \frac{\alpha^2 \cdot k_p}{2\rho^2 \cdot x} - \frac{k_l}{\rho} \cdots (11)$$

$$\alpha = \frac{MW_{SiO_2}}{MW_{O_2} - MW_C} \cong 3 \cdots (12)$$

where x is SiO_2 thickness (m), t is time (s), k_p is the parabolic oxidation rate constant (kg^2/m^4s), ρ is SiO_2 density (kg/m^3), k_l is the linear volatilisation rate constant (kg/m^2s), and MW means molar mass (kg/mol). In Eq. (11), the first term on the right hand means the SiO_2 generation rate by steam oxidation, and the second term means the SiO_2 volatilisation rate.
From Eq. (11), the semi-equilibrium SiO_2 thickness can be obtained by substituting 0 for dx/dt.

$$x = \frac{\alpha^2 \cdot k_p}{2\rho \cdot k_l} \cdots (13)$$

For example, by putting the numerical values of v=0.05m/s, p=2.0MPa, and T=1700K into Eqs. (3), (5), k_p and k_l are calculated as $3.70\times10^{-9} kg^2/m^4s$ and $1.88\times10^{-4} kg/m^2s$, respectively, and by putting these values into Eq.(13) with the numerical value of ρ=2650kg/m^3, the semi-equilibrium SiO_2 thickness (x) is calculated as 16.8nm. From these conditions, the SiO_2 generation rate and SiO_2 volatilisation rate is calculated as 7.08×10^{-5}mm/s. Since cladding thickness of the Step III type fuel is about 0.7mm, potentially that BWR fuel cladding thickness can become 0 at t=2.7h (=0.7/7.08×10^{-5}s). This result suggested that the oxide film volatilisation reaction rate calculated by the second term of the right hand of Eq. (11) may be significantly large at the high pressure condition and some kinds of oxidation-resistant material coating on an outer surface of SiC cladding may be very effective to prevent SiC oxidation and SiO_2 volatilisation reactions. It is also important to improve the accuracies of Eqs. (3), (5) and (6) to simulate oxidation and volatilisation behaviours of SiC fuel. **Fig 7** shows the sensitivity analysis results of SiC without SiO_2 volatilisation. In this case, the margin of depressurisation about doubled compared to **Fig 4**. This result also suggested that prevention of SiO_2 volatilisation is important for SiC fuel. Further investigations are needed for the SiO_2 volatilisation.

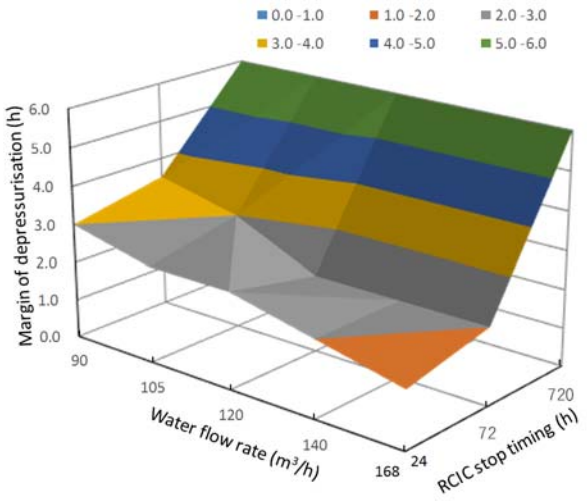

Fig 7. Margin of depressurisation timing
(SiC without oxide film volatilisation (sensitivity analysis))

5. Conclusions

Performance of SiC/SiC composite (SiC) and FeCrAl-ODS steel (ODS) which are applied to

the advanced boiling water reactor (ABWR) were evaluated by the latest MAAP code (MAAP5.05β) for severe accidents (SAs). The analysis results showed the following points.

- ✓ The steam oxidation reaction was effectively suppressed by using the ATFs (i.e. SiC, ODS) instead of the conventional Zircaloy (Zry).
- ✓ The timing of depressurisation could be delayed 0.5-3.0h by using the ATFs compared with the Zry, or the minimum water injection flow rate for the ATFs to prevent core damage could be decreased by about a half compared with the Zry.
- ✓ The prevention of oxide film (SiO_2) volatilisation by use of some kinds of oxidation-resistant material coating may be recommended for SiC cladding.
- ✓ The development of ODS with high Al_2O_3 film stability at high temperature is beneficial for improving performance in accidents.

Acknowledgements

This study is the result of “Development of Technical Basis for Introducing Advanced Fuels Contributing to Safety Improvement of Current Light Water Reactors” carried out under the Project on Development of Technical Basis for Improving Nuclear Safety by Ministry of Economy, Trade and Industry (METI) of Japan.

References

[1] S.C. Johnson, R.E. Henry, C.Y. Paik, “Severe Accident Modeling of a PWR Core with Different Cladding Materials”, Proceedings of ICAPP2012, 12175, Chicago, USA (2012).

[2] L.J. Ott, K.R. Robb, D. Wang, “Preliminary assessment of accident-tolerant fuels on LWR performance during normal operation and under DB and BDB accident conditions”, J. Nucl. Mater., 448, 520-533 (2014).

[3] X. Wu, Y. Zhang, W. Tian, G. Su, S. Qiu, “Preliminary Study on The Effect of Accident Tolerant Fuels on PWR Severe SBO”, Proceedings of ICONE-23, ICONE23-1836, Chiba, Japan (2015).

[4] K.R. Robb, J.W. McMurray, K.A. Terrani, “Severe Accident Analysis of BWR Core Fueled with UO_2/FeCrAl with Updated Materials and Melt Properties from Experiments”, ORNL/TM-2016/237 Rev.0, M2FT-16OR020205042, June 2016.

[5] F. Sebe, M. Yamada, Y. Takeuchi, K. Kakiuchi, K. Okonogi, “Development of Transient and Safety Analysis Method for ATF with SiC”, Proceedings of ICONE-24, ICONE24-60250, Charlotte, NC, USA (2016).

[6] Z.E. Karoutas, R. Schneider, N.R. LaBarge, J. Romeo, P. Xu, “Westinghouse Accident Tolerant Fuel Plant Benefits”, Proceedings of WRFPM2017, A-114, Jeju Island, Korea (2017).

[7] E. van Heerden, C.Y. Paik, S.J. Lee, M.G. Plys, “Modeling of Accident Tolerant Fuel for PWR and BWR using MAAP5”, Proceedings of ICAPP2017, 17737, Fukui and Kyoto, Japan (2017).

[8] J. Wang, M. Mccabe, T.C. Haskin, Y. Wu, G. Su, M.L. Corradini, “Accident Tolerant Cladding Thermal Hydraulic Simulation and Oxidation Kinetic Sensitivity Analysis”, Proceedings of ICONE-25, ICONE25-66523, Shanghai, China (2017).

[9] “Transmittal Document for MAAP5 Code Revision MAAP 5.02”, prepared by Fauske & Associates, LLC, FAI/13-0801, Nov. 2013.

[10] L.L. Snead, T. Nozawa, Y. Katoh, T.S. Byun, S. Kondo, D.A. Petti, “Handbook of SiC properties for fuel performance modeling”, J. Nucl. Mater., Vol.371, 2007, pp.329-377.

[11] K.A. Terrani, B.A. Pint, C.M. Parish, C.M. Silva, L.L. Snead, Y. Katoh “Silicon Carbide Oxidation in Steam up to 2 MPa”, Journal of American Ceramic Society, Vol.97, No.8, 2014, pp.2331-2352.

[12] K.R. Robb, “Analysis of the FeCrAl accidental tolerant fuel concept benefits during BWR station blackout accidents”, Proceedings of NURETH-16, Chicago, IL, August 30-September 4, 2015, pp.1183-1195.

[13] B.A. Pint, K.A. Terrani, Y. Yamamoto, L.L. Snead, “Material Selection for Accident Tolerant Fuel Cladding”, Metallurgical and Materials Transactions E, Vol.2, Issue 3, September 2015, pp.190-196.